Breast Density Classification to aid Clinical Workflow in Breast Cancer Detection using Deep Learning Network

K B Saran
National Institute of Technology, Calicut

G Sreelekha
National Institute of Technology, Calicut

V C Sunitha
Jawaharlal Institute of Postgraduate Medical Education and Research, Pondicherry

***Abstract*—Breast density is an important bio-marker for predicting the risk of breast dancer. Studies have showed that women with dense breast have higher probability of breast cancer. The density, assessed using mammogram images, is a measure of amount of fibro-glandular tissues in a breast and the appearance of it can mask the lesions leading to lesser sensitivity in breast cancer detection. Hence the current clinical workflow for breast detection incorporates a density classification stage which suggest detailed analysis of dense breast using additional imaging modalities like Digital Breast Tomosynthesis (DBT). In this work a breast density classifier using deep neural network architecture employing transfer learning is proposed for the binary classification of breast density to assist in the clinical workflows. The results are evaluated on publicly available databases namely DDSM, MIAS and InBreast. The proposed model outperforms the existing works in the literature giving on an average 96% and 94% accuracy respectively, when tested on DDSM and MIAS database.**

***Index Terms*—Breast density classification, Digital Mammogram, Deep learning, Convolutional Neural Network, Resnet50.**

I. Introduction

Breast cancer (BC) is one of the most common cancers found in women worldwide. According to Globocan 2020 data released by International Agency for Research on Cancer (IARC), the estimated number of new cases of all ages was 2261419 (24.5%) out of 9227484 female studies. In the same study, in India it is observed to be 178361 (26.3%) among 678383 females. In another Indian study, breast cancer has found to be the number one cancer among females with age adjusted rate as high as 25.8 per 100,000 women and mortality 12.7 per 100,000 women [1].

Early detection can reduce the risk of breast cancer through proper and timely treatment methods. Among the various imaging modalities used by radiologists, digital mammography is the most common and cost effective technique for breast cancer screening and diagnosis. Mammograms are captured using low dose X-rays in which two standard views, the craniocaudal (CC) view and the mediolateral oblique (MLO) view of the breast is generated. A women's breast has mainly three types of tissues: fatty tissues, fibrous tissues and glandular tissues. Among the three, the fibrous tissues and glandular tissues are together called as fibro-glandular tissue and are seen as white in a mammogram image and fatty tissues are seen as gray. The relative amount of these tissues in a breast is an important bio-marker for breast cancer screening. It is termed as 'breast density' which gives a comparison between the amount of fibro-glandular tissue and the fatty tissue as seen on a mammogram. To assess the breast density, Breast Imaging Reporting & Data System (BI-RADS) has released a standard reporting system [2] which have four categories of breast composition based on the content of fibro-glandular tissue as given in the Table I. Women in the first two categories (A & B) are having fatty breasts or non-dense and in the other two categories (C & D) are said to have high-density or dense breasts. Studies have showed that women in dense breast category have a higher chance of getting breast cancer [3], [4]. In a mammogram image, dense fibro-glandular tissue can mask a potential cancer because both fibro-glandular tissue and lesions look white on a mammogram. This causes an additional risk in interpreting the mammogram image. Due to these factors and limitations of mammograms, breast density is assessed initially and patients with dense breasts would be advised to undergo additional imaging using Digital Breast Tomosynthesis (DBT).

TABLE I: BI-RADS Reporting system for Breast Density

Category	Breast Composition
A	The breasts are almost entirely fatty
B	There are scattered areas of fibro-glandular density
C	The breasts are heterogeneously dense
D	The breasts are extremely dense

Nowadays computer aided diagnosis (CAD) systems are widely used to assist doctors in the interpretation of medical images. The current systems are based on deep learning methods especially convolutional neural network (CNN). Earlier machine learning algorithms have to be fed with specific features to perform a task. But the CNNs are capable of self extracting the required features from the image. In computer vision applications, CNNs have outperformed the conventional machine learning algorithms. In the proposed method, CNN

based network is used to classify breast mammogram into dense and non-dense as in a clinical procedure of screening. The performance of the method is measured in terms of accuracy, sensitivity, specificity and precision.

II. Related Works in the Literature

Breast density was initially assessed using conventional machine learning algorithms. After the development of deep learning networks for computer vision applications, the latter has almost replaced the conventional methods. One limitation in deep learning method is that, it require large quantity of data for learning process. Availability of such a large medical data is very limited.

Matthews et al., 2020 [5] used Resnet-34 based deep learning model for classifying breast density. Initially the model was trained using full field digital mammogram and evaluated using synthetic mammogram derived from DBT exam. Later, the network was trained using both FFDM and synthetic mammogram. The results were compared and found improvement with adaptation using few synthetic mammography images. They used private data from two different sites for experimentation.

Rampun et al., 2020 [6] proposed an encoding approach, providing a new operator called a local septenary pattern operator. They experimented on various channel encoding techniques for breast density classification in mammograms. They used publically available MIAS and InBreast datasets. They performed pectoral muscle removal from the breast image and extracted a region of interest to reduce false positive rate. Histograms calculated for local binary patterns (LBP), local ternary patterns (LTP), and local quinary patterns were treated as feature vectors. Classification using Random Forest (RF), Support Vector Machine (SVM), k-Nearest Neighbours (k-NN) and Multilayer Perceptron (MLP) were compared.

Lopez-Almazana et al., 2022 [7], proposed a breast density classification method with noisy label regularization and compared the results with radiologists. They used data obtained from a multi-center study. They performed noise removal, breast segmentation using connected component, intensity adjustment and normalization of the grey level before feeding the images to the network for training. The proposed CNN architecture was named Confusion Matrix Convolutional Neural Network (CM-CNN). The network was trained simultaneously with the opinion of three radiologist together with the ground truth distribution. The opinion of each radiologist in density classification is represented by a confusion matrix in which each element is the probability that the radiologist classifies an image in a particular density category. They tested the confusion matrix based method with VGG-19, ResNext4D, DenseNet121, WideResNet50 and EfficientNet-B1 as the base architecture.

Lehman et al., 2019 [8], 2021 [9] trained ResNet-18 deep learning network in Pytorch framework. They assessed the density as both binary classification (dense or non-dense) and across the four BI-RADS categories. The classification using deep learning was evaluated in the clinical environment by comparing the results with that of the radiologist's performance. They studied the clinical acceptance of the deep learning model's density assessment in clinical practice and how the model influence the density assessments.

Kriti et al., 2018 [10] showed the significance of Gabor features in analysing breast density patterns. They used MIAS dataset and from each image, a 200x200 pixel region of interest was extracted from the central part of the breast tissue. Then using 2D Gabor wavelet transform (GWT) the texture information was computed. The performance of Gabor features for density patterns characterization was evaluated using K Nearest Neighbour Classifier, Linear Discriminant Analysis Classifier, Probabilistic Neural Network Classifier, Neural Network Classifier and Support Vector Machine (SVM) Classifier. Among the various classifiers, neural network based classifier performed better.

Kumar et al., 2022 [11] experimented with AlexNet and ResNet-18 by changing the activation function for breast density classification. They used public datasets- MIAS and DDSM and manually extracted ROI of size 224x224 from the center of each mammogram. In the case of DDSM mammograms, ten images are generated using one image and in MIAS dataset, set of twenty images is generated from one sample using augmentation technique. Ciritsis et al., 2018 [12] presented a custom made deep learning model consisting of 13 convolutional layers followed by max-pooling and 4 dense layers with a fully connected softmax layer. The performance of the algorithm was tested by taking a dataset consist of 850 MLO and 882 CC views and another dataset with 100 MLO and 100 CC images. Later the CNN-based classifications were compared with the decision of two radiologists.

The rest of the paper is organized into three sections. In the first section, the dataset and methodology is explained in detail and in the second, results obtained from implementation is discussed. In section V conclusion are drawn out of the research.

III. Material and Methodology

A. Dataset

Many studies are available in literature for breast density classification using both private and public dataset. We utilized three publicly available mammography databases for the experimentation: the Digital Database for Screening Mammography (DDSM) [13], mini-MIAS [14] and InBreast [15].
The DDSM consists of 1370 scanned film mammography studies. It has breast density classification based on BIRADS as ground truth. MIAS contains 322 digitized MLO images

of 161 cases, including benign, malignant lesions and normal cases. It has breast density classified into three classes: fatty, fatty-glandular and Dense-glandular. In INbreast there are a total of 115 cases (410 images). Breast density classification here is based on BIRADS. Since these datasets are having limited number of image sample, augmentation is an essential step for using with deep learning networks. So in our study basic augmentation methods such as rotation, flipping, zooming, intensity and contrast adjustment were performed and generated 8 samples from one sample image.

B. Methodology

1) Preparation of Data: The DDSM and INbreast data were in DICOM format and MIAS data were in PGM format. So the initial step was to get the pixel information from the DICOM file. Later, images were passed through the preprocessing stage. A 3x3 median filter is applied to remove the digitization noise. Since the fibro-glandular tissues are indicating the density of breast, it has to be enhanced properly. So an adaptive histogram equalization named Contrast Limited Adaptive Histogram Equalization (CLAHE) [16] is performed. CLAHE was widely used to improve low-contrast medical images [17].

a) Contrast Limited Adaptive Histogram Equalization: CLAHE is a contrast enhancement technique, which works on small areas of an image called 'tiles' or 'block'. By this local area approach, it is capable of preventing contrast over-amplification. CLAHE has two parameters to control the contrast and intensity. They are clip limit and block size. The CLAHE technique divides an input original image into non-overlapping blocks as defined in the block size. Then it clips the histogram of each block at a predefined value and redistribute it before computing the Cumulative Distribution Function (CDF). By varying the clip limit, image intensity is adjusted and by varying the block size, the dynamic range is adjusted, and thereby the image contrast. For the processing of mammogram images, the clip limit chosen is 10 and block size 5x5. The resulting image after CLAHE is shown in Fig.1.

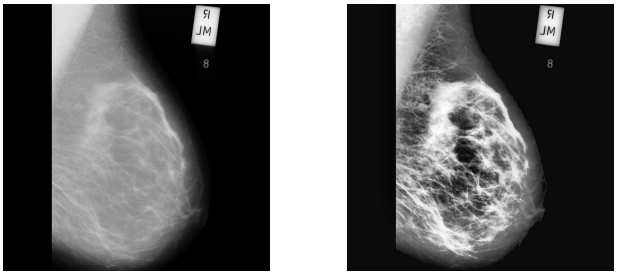

(a) Original Image (b) After CLAHE

Fig. 1: Example for Mammogram image after applying CLAHE

b) Morphological Operations: A typical mammogram include breast image as well as annotations such as the type of view, date of image acquisition, patient identification. These details are unwanted for our training purposes. So it is necessary to remove these informations and segment only the breast section. Before the segmentation, morphological operations were performed [18]. In morphological operations, top-hat and black-hat transforms were used to extract small details from the mammogram image. Top-hat transform is obtained by taking the difference between input image and its opening by the structuring element, while the black-hat transform is the difference between the closing and the input image. The process is given in Equ. 1 and Equ. 2.

$$Tophat, T_w(f) = f - (f \circ b) \tag{1}$$

$$Blackhat, T_b(f) = (f \bullet b) - f \tag{2}$$

Final transformed image is obtained as;

$$T(f) = f + T_w(f) - T_b(f) \tag{3}$$

where, f is the given image, $\circ$ denotes opening operation, b is the structuring element and $\bullet$ denotes the closing operation.

After the morphological operation, another filter known as Gabor filter is applied to enhance the fibro-glandular tissues [10], [19]. In image processing, Gabor filter is used for edge detection, texture classification and feature extraction. Since the quantity of fibro-glandular tissues are reflecting the breast density, it is essential to enhance it.

c) Gabor filter: Gabor filters are special type of bandpass filters, which allow a band of frequencies and reject others. It is obtained by modulating a sinusoidal signal of particular frequency and orientation with a Gaussian function. To enhance texture feature in an image, a bank of Gabor filters of different orientations are used. The filter has a real and an imaginary component represented in orthogonal directions.
The mathematical representation of Gabor function is given in Equ. (4) and Equ. (5).

$$g(x, y, \lambda, \theta, \psi, \sigma, \gamma) = \exp^{(-\frac{x'^2 + \gamma^2 y'^2}{2\sigma^2})} cos(2\pi \frac{x'}{\lambda} + \psi) \tag{4}$$

$$g(x, y, \lambda, \theta, \psi, \sigma, \gamma) = \exp^{(-\frac{x'^2 + \gamma^2 y'^2}{2\sigma^2})} sin(2\pi \frac{x'}{\lambda} + \psi) \tag{5}$$

The Equ. (4) and Equ. (5) are real and imaginary parts of Gabor filter respectively with

$$x' = xcos\theta + ysin\theta \tag{6}$$

$$y' = -xsin\theta + ycos\theta \tag{7}$$

In the filter function, λ represents the wavelength of the sinusoid, θ is the orientation, ψ is the phase offset, σ is the standard deviation of the Gaussian envelope and γ is the spatial aspect ratio that specifies the ellipticity of the support of the Gabor function. By varying the parameters, $\lambda, \theta, \psi, \sigma$ and γ, we can get different filters that forms a filter bank [20]. In the

implementation, except θ, all other parameters are fixed and edges at various orientations are highlighted. The resultant of Gabor filtering applied on mammogram image is shown in Fig. 2.

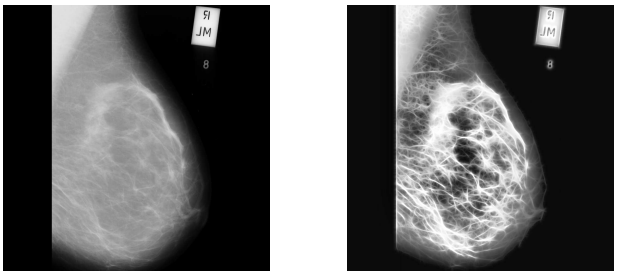

(a) Original Image (b) Output of Gabor Filter

Fig. 2: Example for Mammogram image after Gabor Filtering. It can be seen that the fibro-glandular tissues are highlighted.

As the last step, image segmentation is performed to extract only the breast region. Otsu threshold based segmentation is used in the implementation. Fig 3 shows the segmented breast region of a sample image by removing annotations. This image is given to the deep learning network after augmentation as mentioned in the section III.A.

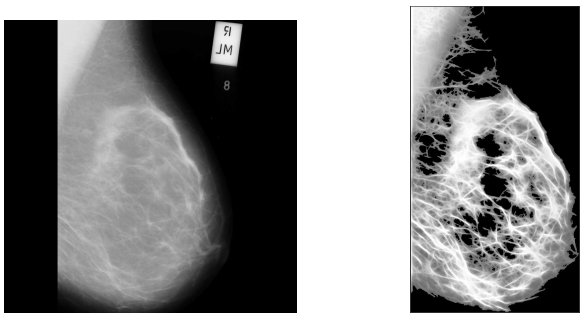

(a) Original Image (b) Segmented Image.

Fig. 3: Example for Mammogram image after segmentation

2) Training and Testing of Convolutional Neural Network: The deep learning model and training procedures were implemented using the PyTorch framework in Google colab with Tesla T4 GPU. The available data were split in 80:20 ratio as training and testing set respectively. Table II describe the details of dataset after augmentation.

TABLE II: Number of images in each density class after augmentation

Database Name	Number of images in each BI-RADS class
InBreast	A:1088 , B:1168, C:792, D: 232
MIAS	Dense-Glandular: 896, Fatty: 848, Fatty-Glandular: 832
DDSM	A:1896 , B:4224, C:3200, D: 1640

In this implementation, transfer learning approach is used with ResNet50 deep learning network [21]. As the name indicates, it is a 50 layer network consist of:

- Conv-1 **(1 Layer)**: One 7×7 kernel convolution alongside 64 other kernels with a stride of 2.
- **(1 Layer)** One max pooling layer with a stride of 2
- Conv-2 **(9 Layers)**: One 3×3, 64 kernel convolution, one 1×1, 64 kernels, another one with 1×1, 256 kernels. These 3 layers are repeated 3 times.
- Conv-3 **(12 Layers)**: One 1×1, 128 kernels, one 3×3, 128 kernels, and one 1×1, 512 kernels, iterated 4 times.
- Conv-4 **(18 Layers)**: One 1×1, 256 kernals, one 3×3, 256 kernals and one 1×1, 1024 kernals, iterated 6 times.
- Conv-5 **(9 Layers)**: One 1×1, 512 kernals, one 3×3, 512 kernals, and one 1×1, 2048 kernals iterated 3 times.
- Averaging Polling Layer and 1000 node fully connected layer with Softmax activation.

Resnet50 provides a novel way to add more convolutional layers to a CNN, without running into the vanishing gradient problem, using the concept of shortcut connections. A shortcut connection "skips over" some layers, converting a regular network to a residual network. ResNet50 accepts images with size 224x224, so the images were resized to suit with the network's input layer. The loss function used was cross-entropy and the training was optimized using Adaptive Moment Estimation (Adam) optimizer. The number of epochs were decided based on the variation of training and validation loss and a batch size of 32 was selected for training.

The learning rate is an important hyper parameter that decides the step size of gradient descent in reaching the minima or the amount that the network weights are getting updated. To find the learning rate, a mini batch of data is fed to the network with a small value for the learning rate and the learning rate is increased gradually by monitoring the loss function at each iteration [22]. Then a graph is plotted between loss function and learning rate. Based on the plot, optimal learning rate is selected from the region where the loss function is changing linearly. Fig.4 shows the learning rate v/s loss plot for Inbreast dataset which shows an optimal learning rate value indicated in orange colour circle.

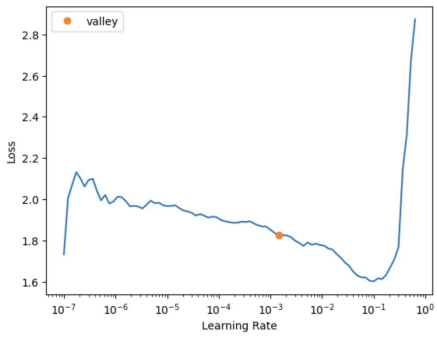

Fig. 4: Plot for learning rate v/s loss function

This learning rate is used to train only the last layer by keeping all other layers frozen for some epochs. Later again the learning rate is calculated based on the same procedure. Then the initial layers were also trained in such a way that learning rates are incremented linearly going from the first

TABLE III: Summary of breast density classification performance using ResNet50. (Fatty [BI-RADS A and B], Dense [BI-RADS C and D])

Dataset	Accuracy	Sensitivity	Precision	Specificity	F1-Score
DDSM	0.96 (Binary Class)	Fatty: 0.97, Dense: 0.95	Fatty: 0.96, Dense: 0.95	Fatty: 0.95, Dense: 0.96	Fatty: 0.96, Dense: 0.95
MIAS	0.94 (3 class)	Dense: 0.94, Fatty: 0.95, Glandular: 0.92	Dense: 0.94, Fatty: 0.98, Glandular: 0.89	Dense: 0.96, Fatty: 0.98, Glandular: 0.89	Dense: 0.94, Fatty: 0.96, Glandular:0.90
InBreast	0.91 (Binary Class)	Fatty: 0.96, Dense: 0.81	Fatty: 0.91, Dense: 0.91	Fatty: 0.907, Dense: 0.908	Fatty: 0.93, Dense: 0.85
DDSM (Without Pre-processing)	0.87 (Binary Class)	Fatty: 0.90, Dense: 0.85	Fatty: 0.87, Dense: 0.88	Fatty: 0.84, Dense: 0.89	Fatty: 0.88, Dense: 0.86

TABLE IV: Comparison of breast density classification using ResNet18, ResNet50 and ResNet101 with DDSM Dataset

Dataset	Accuracy	Sensitivity	Precision	Specificity	F1-Score
ResNet18	0.91	Fatty: 0.91, Dense: 0.92	Fatty: 0.94, Dense: 0.88	Fatty: 0.92, Dense: 0.91	Fatty: 0.92, Dense: 0.90
ResNet50	0.96	Fatty: 0.97, Dense: 0.95	Fatty: 0.96, Dense: 0.95	Fatty: 0.95, Dense: 0.96	Fatty: 0.96, Dense: 0.95
ResNet101	0.93	Fatty: 0.93, Dense: 0.94	Fatty: 0.95, Dense: 0.90	Fatty: 0.94, Dense: 0.92	Fatty: 0.94, Dense:0.92

to last layer, ensuring the early layers are trained at a lower learning rate when compared to later layers.

IV. Result and Discussion

The ResNet50 was trained with three different digital mammogram dataset. In clinical procedure, it is required to classify the breast into fatty and dense. So to aid that, the training is done for binary class. In the dataset except for MIAS, the BIRADS A& B together are taken as fatty and C& D together as dense. Since MIAS dataset has three classes, it is considered as it is. Fig. 5 shows the variations of training and validation losses for each epoch.

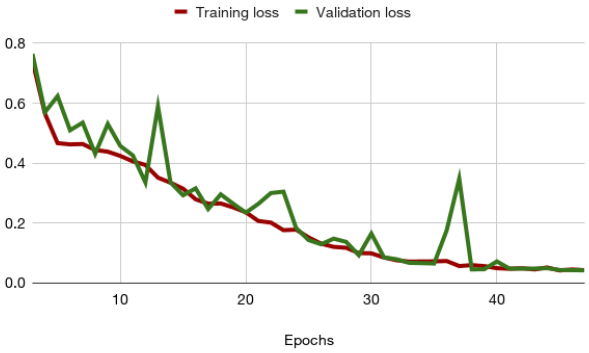

Fig. 5: Plot showing the training and validation loss for each epoch

The performance of the network is measured in terms of Accuracy, Precision, Sensitivity, Specificity and F1-Score after plotting the confusion matrix. It is easy to understand the True positive, True negative, False positive and False negative from the confusion matrix. Fig. 6 shows the variation of F1-score obtained during training and validation process.

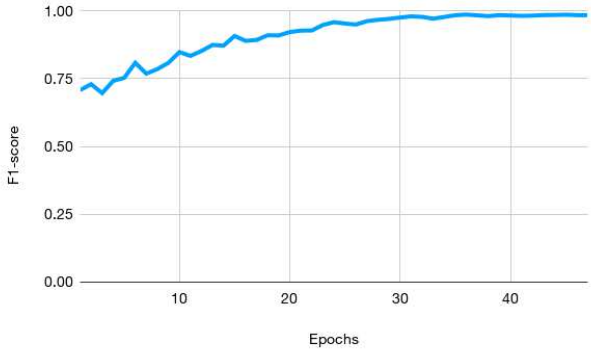

Fig. 6: Plot F1-score variations during training and validation

Table III summarizes the performance ResNet50 for the the three datasets. It can be observed that the accuracy obtained for DDSM, MIAS and InBreast dataset were 0.96, 0.94 and 0.91 respectively. The F1-score indicates a good balance between the precision and sensitivity. Though there is a decrease in the performance of the network for InBreast dataset, it is showing good results in comparison with other works in the literature. Last row in the table shows the results obtained when the network is trained with images which are not passed through the preprocessing stages. The result shows that preprocessing stage plays a significant role in the network performance. A comparison is also made with two other variants of ResNet architecture, ResNet18 and ResNet101 which is shown in Table VI. According to that, ResNet50 provides better result for the DDSM dataset in the breast density classification.
Table V compares the proposed method with the previous works in the literature. Accuracy is considered for comparison and it can be observed that the proposed method with ResNet50 gives better result.

TABLE V: Comparative analysis between proposed works and previous works in literature in terms of accuracy

Reference	Method	Accuracy
Matthews et al., [5], 2020	ResNet34	0.911
Rampun et al., [6], 2020	Multilayer Perceptron	0.833
Almazan et al., [7], 2022	CM-CNN	0.84
Lehman et al., [8], 2019	ResNet18	0.87
Kumar et al., [11], 2022	ResNet18	0.923
Proposed Method	**ResNet50**	**0.96**

V. Conclusion

A binary breast density classifier using transfer learning approach is proposed in this work. A ResNet50 architecture with data augmentation is tested on the publicly available datasets to have a fare comparison with the existing works in literature. Various pre-processing stages that enhanced the features of interest such as fibro-glandular cells along with data augmentation gave a better result compared to the existing works. Appropriate tuning of the parameter models also augmented better results. The main aim of this experimentation is to aid in the clinical workflow for breast cancer screening. A screening based on breast density will help to reduce the cost of disease diagnosis and to increase the accuracy of breast cancer detection. So this work can be extended after clinical validation to improve the assessment parameters and to make the sensitivity close to hundred as required by any screening system.

References

[1] Malvia S, Bagadi SA, Dubey US, Saxena S. Epidemiology of breast cancer in Indian women. Asia Pac J Clin Oncol. 2017 Aug;13(4):289-295. doi: 10.1111/ajco.12661. Epub 2017 Feb 9. PMID: 28181405.

[2] Sickles, Edward A., Carl J. D'Orsi, Lawrence W. Bassett, Catherine M. Appleton, Wendie A. Berg, and Elizabeth S. Burnside. "Acr bi-rads® mammography." ACR BI-RADS® atlas, breast imaging reporting and data system 5 (2013): 2013.

[3] Boyd, N.F., Byng, J.W., Jong, R.A., Fishell, E.K., Little, L.E., Miller, A.B., Lockwood, G.A., Tritchler, D.L. and Yaffe, M.J., 1995. Quantitative classification of mammographic densities and breast cancer risk: results from the Canadian National Breast Screening Study. JNCI: Journal of the National Cancer Institute, 87(9), pp.670-675.

[4] Ali, E.A., Raafat, M. Relationship of mammographic densities to breast cancer risk. Egypt J Radiol Nucl Med 52, 129 (2021). https://doi.org/10.1186/s43055-021-00497-y.

[5] Matthews, Thomas P., Sadanand Singh, Brent Mombourquette, Jason Su, Meet P. Shah, Stefano Pedemonte, Aaron Long et al. "A multisite study of a breast density deep learning model for full-field digital mammography and synthetic mammography." Radiology: Artificial Intelligence 3, no. 1 (2020): e200015.

[6] Andrik Rampun, Philip J. Morrow, Bryan W. Scotney, Hui Wang, Breast density classification in mammograms: An investigation of encoding techniques in binary-based local patterns, Computers in Biology and Medicine, Volume 122, 2020, 103842, ISSN 0010-4825, https://doi.org/10.1016/j.compbiomed.2020.103842.

[7] Lopez-Almazan, H., Pérez-Benito, F.J., Larroza, A., Perez-Cortes, J.C., Pollan, M., Perez-Gomez, B., Trejo, D.S., Casals, M. and Llobet, R., 2022. A deep learning framework to classify breast density with noisy labels regularization. Computer Methods and Programs in Biomedicine, 221, p.106885.

[8] Lehman, C.D., Yala, A., Schuster, T., Dontchos, B., Bahl, M., Swanson, K. and Barzilay, R., 2019. Mammographic breast density assessment using deep learning: clinical implementation. Radiology, 290(1), pp.52-58.

[9] Dontchos, Brian N., Adam Yala, Regina Barzilay, Justin Xiang, and Constance D. Lehman. "External validation of a deep learning model for predicting mammographic breast density in routine clinical practice." Academic Radiology 28, no. 4 (2021): 475-480.

[10] Kriti, Jitendra Virmani, and Ravinder Agarwal. "Evaluating the efficacy of Gabor features in the discrimination of breast density patterns using various classifiers." Classification in BioApps: Automation of Decision Making (2018): 105-131.

[11] Kumar, Indrajeet, Abhishek Kumar, VD Ambeth Kumar, Ramani Kannan, Vrince Vimal, Kamred Udham Singh, and Mufti Mahmud. "Dense tissue pattern characterization using deep neural network." Cognitive computation 14, no. 5 (2022): 1728-1751.

[12] Ciritsis, Alexander, Cristina Rossi, Ilaria Vittoria De Martini, Matthias Eberhard, Magda Marcon, Anton S. Becker, Nicole Berger, and Andreas Boss. "Determination of mammographic breast density using a deep convolutional neural network." The British journal of radiology 92, no. 1093 (2019): 20180691.

[13] Sawyer-Lee, R., Gimenez, F., Hoogi, A., and Rubin, D. (2016). Curated Breast Imaging Subset of Digital Database for Screening Mammography (CBIS-DDSM) (Version 1) [Data set]. The Cancer Imaging Archive. https://doi.org/10.7937/K9/TCIA.2016.7O02S9CY.

[14] Suckling, J., Parker, J., Dance, D. et al. (2015). Mammographic Image Analysis Society (MIAS) database v1.21. [Dataset]. Apollo - University of Cambridge Repository. https://www.repository.cam.ac.uk/handle/1810/250394

[15] Moreira IC, Amaral I, Domingues I, Cardoso A, Cardoso MJ, Cardoso JS. INbreast: toward a full-field digital mammographic database. Acad Radiol. 2012 Feb;19(2):236-48. doi: 10.1016/j.acra.2011.09.014. Epub 2011 Nov 10. PMID: 22078258.

[16] Zuiderveld, Karel. "Contrast limited adaptive histogram equalization." Graphics gems (1994): 474-485.

[17] Mayya V, S S, Kulkarni U, Surya D and Acharya U. (2023). An empirical study of preprocessing techniques with convolutional neural networks for accurate detection of chronic ocular diseases using fundus images. Applied Intelligence. 53:2. (1548-1566).

[18] Saber, Abeer, Mohamed Sakr, Osama M. Abo-Seida, Arabi Keshk, and Huiling Chen. "A novel deep-learning model for automatic detection and classification of breast cancer using the transfer-learning technique." IEEE Access 9 (2021): 71194-71209.

[19] R. Roslan and N. Jamil, "Texture feature extraction using 2-D Gabor Filters," 2012 International Symposium on Computer Applications and Industrial Electronics (ISCAIE), Kota Kinabalu, Malaysia, 2012, pp. 173-178, doi: 10.1109/ISCAIE.2012.6482091.

[20] Li, Yue, Zilong He, Xiangyuan Ma, Weimin Xu, Chanjuan Wen, Hui Zeng, Weixiong Zeng et al. "Architectural distortion detection in digital breast tomosynthesis with adaptive receptive field and adaptive convolution kernel shape." In Medical Imaging 2021: Computer-Aided Diagnosis, vol. 11597, pp. 592-599. SPIE, 2021.

[21] He, Kaiming, Xiangyu Zhang, Shaoqing Ren, and Jian Sun. "Deep residual learning for image recognition." In Proceedings of the IEEE conference on computer vision and pattern recognition, pp. 770-778. 2016.

[22] Jordan, Jeremy. "Setting the learning rate of your neural network." Data Science (2018): 1-30.